Korean J. Chem. Eng., **26**(2), 496-499 (2009)

Effect of laser beam focusing point on AFM measurements

Younghun Kim*,†, Young In Yang, Inhee Choi**, and Jongheop Yi****

*Department of Chemical Engineering, Kwangwoon University, Seoul 139-701, Korea
**School of Chemical and Biological Engineering, Seoul National University, Seoul 151-742, Korea
(*Received 9 June 2008 • accepted 29 September 2008*)

Abstract−The optical beam deflection method, which is used in AFM to obtain surface images, may distort the resulting image. The flexible and long cantilever is easily overdamped by the laser radiation pressure, resulting in steady deflection of the cantilever (<1 nm). This deflective force distorts the image and influences the force-distance (F-D) curve. The present study investigated the effect of laser radiation pressure on image distortion. As a proof-of-concept test, two grating samples (with step heights of 150 and 18 nm for TGX01 and TGZ01, respectively) were examined with an NSC36 series cantilever in air and water media.

Key words: Atomic Force Microscopy, Image Distortion, Laser Beam, Radiation Pressure

INTODUCTION

The atomic force microscope (AFM) has emerged as a useful tool for microscopic reading of surface morphology [1], lithographic writing of nanopatterns onto substrate [2], and spectroscopic measuring of conductance between two electrodes [3]. Quality surface images with high resolution are of fundamental importance to many fields of research, including surface science, materials engineering, biochemistry and biology. Surface-morphology analysis of an unknown sample does not always provide a trustworthy, non-distorted and accurate image of the sample. Image quality is affected by the analysis conditions, such as scan mode, scan rate, type of cantilever and liquid media, and relative humidity. For example, in liquid media the dependence of image distortion on fluid properties (kinematic viscosity) has been studied by using the edge friction force obtained in lateral images [1,4]. In addition, the effects of the properties of the spring and tip used to probe the sample surface on image quality and force measurement have been extensively studied [5-7].

In a typical AFM setup, the optical beam deflection method is used to obtain surface images with a flexible cantilever. A laser beam is focused on the backside of the cantilever and the reflected beam is detected by using a quartered photodiode. A beam of light exerts sufficient radiation pressure to move a microstructure, as confirmed by experimental evidence from several studies [8,9]. It is possible to determine height deviation of the laser reflected on the photodiode, along with the laser focusing position on the cantilever. In particular, the degree of cantilever deflection may vary with the laser beam focusing position on the cantilever. Pal and Ghosh investigated optical pressure resulting from a laser beam on a singly clamped cantilever, based on the assumption that the length of the cantilever is an order of magnitude greater than the size of the laser spot [8]. In their study, an optimal reflection position, which is highly responsive to the sample surface, exists on the cantilever.

Herein, we describe variation in image distortion with laser beam focusing point in liquid and ambient AFM on a singly clamped cantilever. Results of a model to test for deviation in the morphological image of two grating samples obtained in air and water media are also discussed. The open liquid-cell AFM used in this study allowed easy exchange and prevented solution overflow. The noise levels (root-mean-square) for mica in air and water were used to monitor image reliability.

EXPERIMENTAL SECTION

As illustrated in Fig. 1(a), an open liquid-cell system was used in conjunction with a commercial AFM instrument (XE-100, PSIA, Korea). To minimize intrinsic distortion of the apparatus, an independent z-scanner was used, which also eliminated the problem of x-z cross coupling that is inherent in conventional AFM [10]. The assembled system was tested for image distortion by using standard grating samples (TGX01 and TGZ01, MikroMasch, Estonia) in air and water in the contact mode. To investigate the dependence of sample roughness on the focusing point, two different grating samples were used. The TGX01 (chess-board pattern) and TGZ01 (striped pattern) step heights were ca. 150 and 18 nm, respectively. The pitch size of both grating samples was 3 μm. A 650 nm InGaAlP diode laser beam with a power output of 5 mW (QL65D5S, QSI Laser, Korea) was normally incident to the cantilever. The relative humidity (RH) in air condition has an influence on the F-D curve

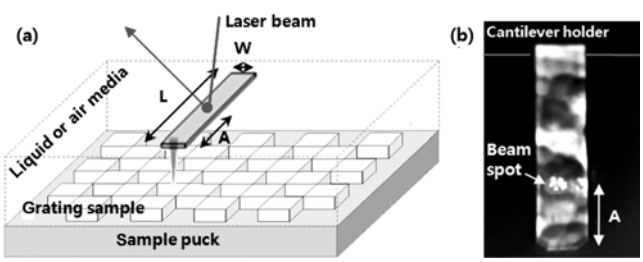

Fig. 1. (a) Schematic of image analysis of grating samples, and (b) picture of the backside of the NSC36 cantilever used in this study.

†To whom correspondence should be addressed.
E-mail: korea1@kw.ac.kr

Table 1. Operation parameters of cantilevers and grating samples

Parameters	Value or range	Unit	Remarks
Cantilever length, L	110±5; 90±5; 130±5	μm	NSC36A; NSC36B; NSC36C
Spring constant, k	0.95; 1.75; 0.60	N/m	NSC36A; NSC36B; NSC36C
Cantilever width, W	35±3	μm	NSC36
Beam spot size, w	20±5	μm	Diode laser
Point of incident laser, A	0-110; 0-90; 0-130	μm	NSC36A; NSC36B; NSC36C
Height of grating sample, h	150±5; 18±1	nm	TGX01; TGZ01
Pitch of grating sample	3	μm	TGX01 and TGZ01

obtained. Therefore, the experiment for ambient air was performed in a humidity-controlled box equipped with an AFM, and RH was fixed to 40±10%.

To find the optimal reflection position of the laser beam on the cantilever, focusing point (A) was adjusted over the full-length of the cantilever, as shown in Fig. 1(b). An NSC36 (MikroMasch, Estonia) series was selected as the contacting cantilever, and used most frequently in contact mode. Measurements with the different cantilevers were repeated ten times at five focusing points. Detailed information regarding the cantilevers and grating samples is summarized in Table 1.

RESULTS AND DISCUSSION

A 650-nm, 5-mW laser beam had sufficient power to optically deflect the flexible and singly clamped cantilever. Assuming 100% efficiency of a light source, the laser energy was estimated by using the simple equation ($E=h\nu=hc/\lambda$) to be ca. 3.1×10^{-19} J. The cantilever acted as an elastic spring; thus, its restoring force can be estimated from Hooke's law ($F=-kx$). The potential energy stored in a spring is given by ($U=1/2kx^2$). If the energy of the laser is similar to the energy of the spring, the distance (x) that the spring is stretched or compressed from the equilibrium position by the laser beam can be calculated. Based on the operation parameters shown in Table 1, the deflected distance of the NSC36A, NSC36B, and NSC36C cantilevers was 0.8, 0.6, 1.0 nm, respectively. The results of this simple calculation showed that optical deflection of a cantilever by a laser beam is possible.

When the cantilever was immersed in liquid media, the deflected distance of the cantilever was reduced. This phenomenon can be interpreted as follows. The van der Waals force that arises from the interaction between tip and sample can be quantified by using the Hamaker constant. This constant is dependent on the system characteristics, such as the material and environmental media [11]. Both the cantilever and grating sample were comprised of SiO_2. The Hamaker constant in a SiO_2/vacuum/SiO_2 system is approximately 5.5×10^{-20} J, while that in a SiO_2/water/SiO_2 system is 1.6×10^{-21} J [12]. Therefore, cantilever deflection in water media by laser radiation and van der Waals attraction will be slightly less than deflection in a vacuum.

In addition, the optimal deflection point (A_{opt}), which represents the position on the cantilever most sensitive to laser radiation pressure, can be determined from the following equation. Detailed information regarding the equation can be found in reference [8]. Let y_1 and y_2 represent the left- and right-terms of the equation, respectively.

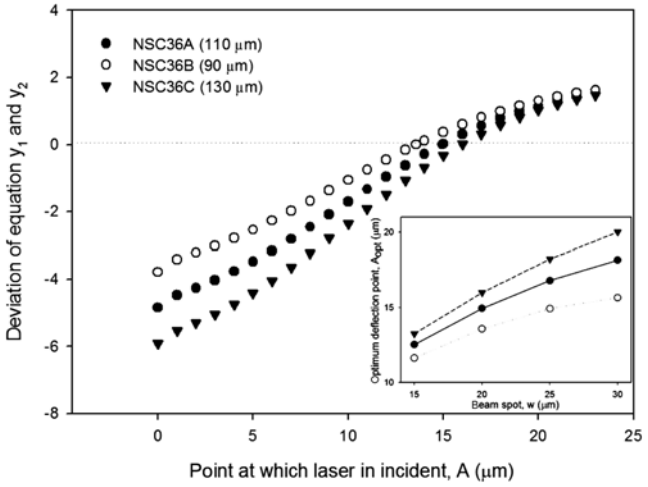

Fig. 2. Change in cantilever deflection with laser beam focusing point for different cantilevers. Inset figure is the optimal deflection point with size of beam spot on the cantilever.

$$\frac{4}{3}\sqrt{\frac{2}{\pi}}\frac{L}{w}e^{-2A/w}=1+\mathrm{erf}\sqrt{2A/w}$$

Where, L, w, and A are cantilever length, beam spot size, and point of the incident laser, respectively. When the deviation between y_1 and y_2 is zero, point (A), at which the laser is incident on the cantilever, becomes A_{opt}. As shown in Fig. 2, A_{opt} varies with cantilever type, exact cantilever length, and spring constant. The long cantilever (NSC36C) with a small spring constant is more flexible than NSC36B, and A_{opt} shifted slightly towards the cantilever holder from the end of cantilever. The ratios of A to L for the NSC36 series were 0.136, 0.151, and 0.123, respectively. In particular, for a 20-μm beam spot, the appropriate laser beam focusing points relative to the length of the entire cantilever were ca. 14, 13, and 12% zone for NSC36A, NSC36B, and NSC36C, respectively. Since the spot size of the incident beam has a deviation of ±5 μm, A_{opt} was calculated by using beam spot size as shown in the inset of Fig. 2.

As a proof-of-concept test, the grating samples with step heights of 150 and 18 nm were scanned in water and air at five focusing points. Figs. 3 and 4 show the cross-sectional 3D images of TGX01 in water and TGZ01 in air. The height of the grating sample with the large height deviation (TGX01) varied with the laser beam focusing point in the cross-sectional analysis. However, the cross-sectional height of TGZ01 in Fig. 4 was not highly dependent on the

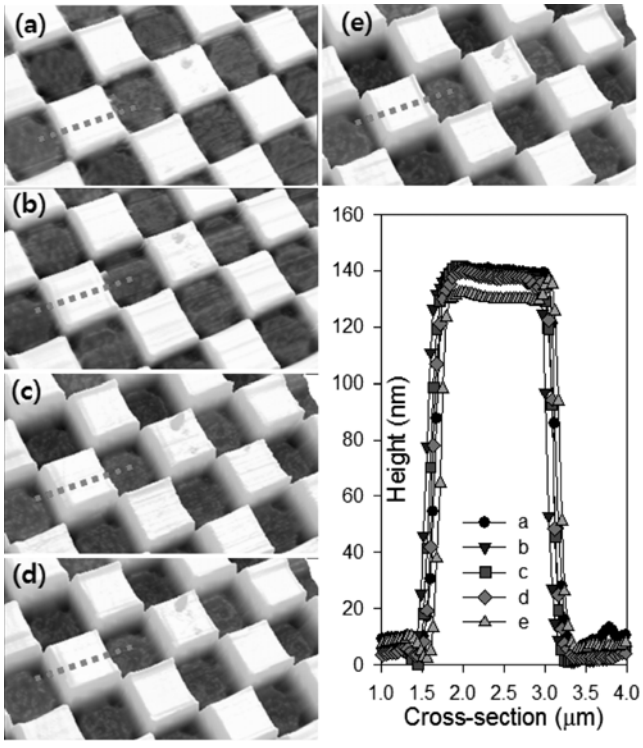

Fig. 3. Cross-sectional 3D images of grating sample (TGX01) in water media were analyzed with the laser positioned (a) 19, (b) 38, (c) 58, (d) 77, and (e) 97 μm. The NSC36C cantilever was used herein.

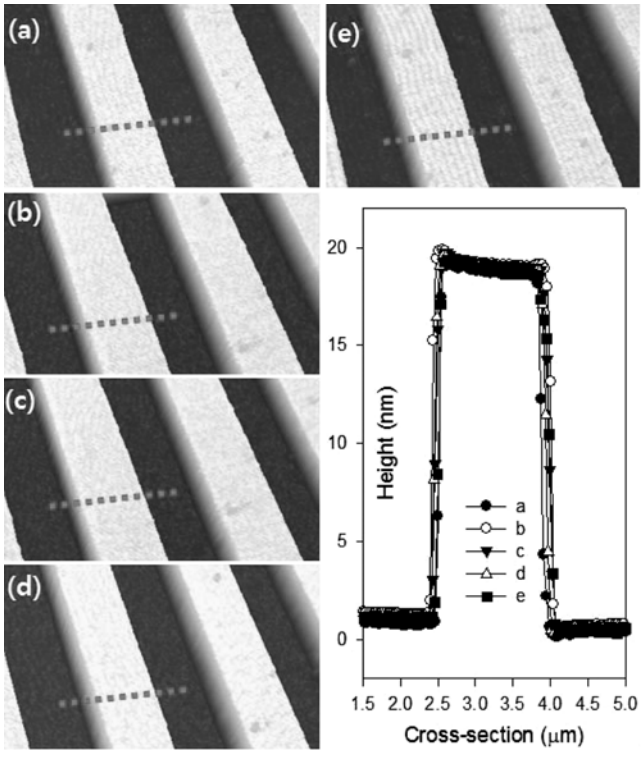

Fig. 4. Cross-sectional 3D images of grating sample (TGZ01) in air media were analyzed with the laser positioned at (a) 19, (b) 38, (c) 58, (d) 77, and (e) 97 μm. The NSC36C cantilever was used herein.

laser focusing point on the cantilever. The height deviations (Δh) of TGX01 and TGZ01 were 5 and 0.5 nm, respectively. It should be noted that the influence of the laser focusing point on the cantilever on the resulting image (especially the height information) is as great as the influence of sample surface (e.g., coarse and rough surface). This feature may result in erroneous interpretation of AFM data for unknown samples. When thin organics (<5 nm thick) are immobilized on a rough surface with significant height variance, the height information analyzed at different focusing points may vary from that obtained at A_{opt}. Therefore, rough surfaces should be analyzed with the laser focusing point positioned at A_{opt} on the cantilever, if possible. However, in the case of smooth surfaces, the correlation between topographic data and the laser focusing point was not as strong. In addition, the height deviation of TGX01 was reduced when a stiffer cantilever with a high spring constant (NSC36B) was used in place of NSC36C. Because a short cantilever with a high spring constant is less flexible, NSC36B has higher resistance to laser radiation pressure than NSC36C.

Analysis of TGX01 in air and TGZ01 in water yielded results similar to those presented in Fig. 3 (TGX01 in water) and Fig. 4 (TGZ01 in air). In previous studies, the dependence of image distortion on fluid properties has been studied by using the edge friction force obtained in lateral images [1,4]. Image distortion in liquid media is strongly dependent on the kinematic viscosity of the liquid. The kinematic viscosities of air and water are nearly identical, and image distortions in air and water also are similar to each other. If a liquid with high kinematic viscosity had been used instead of water, different effects on image distortion might have been observed.

The relationship between image distortion and focusing point could be examined by force-distance (F-D) analysis, which is routinely used to determine elasticity, adhesion energy, and degree of hydrophobicity. The most interesting regions of F-D curves are the non-contact regions containing the jump-to-contact and jump-off-contact points, which provide information about the attractive and repulsive forces both before and after contact. In particular, the measured force at the jump-off-contact point relates to the contact adhesive stress, from which the adhesion energy can easily be obtained by integration of the triangular area at this point [13]. As shown in

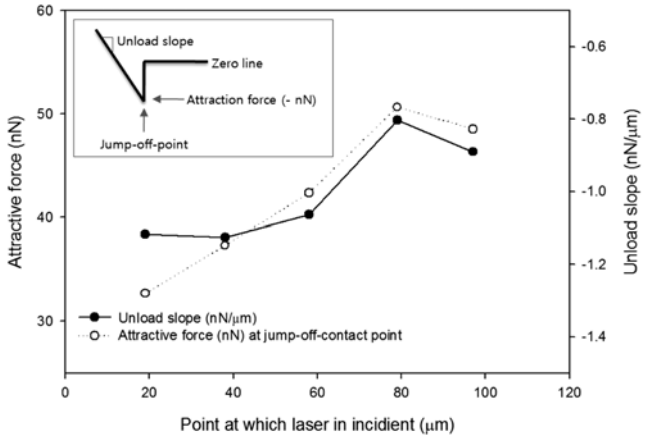

Fig. 5. Force-distance (F-D) curves. The attractive force at the jump-off-point and the unload slope were analyzed at different laser points. The inset is a general F-D curve.

Fig. 5, the attractive force at the jump-off-contact point in the F-D curve was obtained from analysis of TGX01 at different laser focusing points on NSC36C in air media. The attractive force at the jump-off-contact point was negative, ranging from 30 to 50 nN. The attractive force increased with focusing point (A) up to the fourth point. The unload slope showed a pattern similar to that of the attractive force. As the laser beam moved inside the cantilever, the degree of cantilever deflection by laser radiation pressure decreased; thus, the apparent attraction force between the probe tip and sample surface increased. The point to keep in mind here, however, is that adhesion force in air is not commonly reported in the literature given the effects of capillary forces, which vary with humidity and type of cantilever. Therefore, adhesion data obtained in this work might be over measured as 67% increase. However, this result suggests that the attractive term in the F-D curve is affected by the laser focusing point on the cantilever.

CONCLUSIONS

The light source used in the optical beam deflection method, which is used to capture surface images in AFM analysis, has sufficient potential to deflect a singly clamped flexible cantilever. This phenomenon may influence distortion of the image and F-D curve, giving erroneous data for unknown samples. When the height variance of the sample surface was large, the measured height varied with the laser focusing point on the cantilever. This feature was much more prominent with the NSC36C cantilever as compared to the short NSC36B cantilever with a high spring constant. However, for smooth surfaces, image distortion was less dependent on laser focusing point. The point to keep in mind is that the effect of the laser beam for AFM image and F-D curve could be different with cantilever shape (rectangular or triangular), deflection sensitivity, spring constant, and so on.

ACKNOWLEDGMENT

We are grateful to the Korea Research Foundation Grant (KRF-2007-331-D00094) and Research Grant of Kwangwoon University in 2008.

REFERENCES

1. Y. Kim, S. K. Kang, I. Choi, J. Lee and J. Yi, *Appl. Phys. Lett*., **88**, 173121 (2006).
2. I. Choi and J. Yi, *Korean J. Chem. Eng*., **25**, 386 (2008).
3. Y. Kim, I. Choi, S. K. Kang, J. Lee and J. Yi, *Appl. Phys. Lett*., **86**, 073113 (2005).
4. Y. Kim and J. Yi, *J. Phys. Chem. B*, **110**, 20526 (2006).
5. J. L. Hutter and J. Bechhoefer, *Rev. Sci. Instrum*., **64**, 1868, (1993).
6. R. E. Jones and D. P. Hart, *Tribol. Int*., **38**, 335 (2005).
7. Y. Sun and J. H. L. Pang, *Nanotechnology*, **17**, 933 (2006).
8. S. Pal and A. K. Ghosh, *Electronic Lett*., **42**, 580 (2006).
9. D. Dragoman and M. Dragoman, *Appl. Opt*., **38**, 6773 (1996).
10. J. Kwon, J. Honh, Y.-S. Kim, D.-Y. Lee, S. Lee and S. Park, *Rev. Sci. Instrum*., **74**, 4378 (2003).
11. C. Argento and R. H. French, *J. Appl. Phys*., **80**, 6081 (1996).
12. H. D. Ackler, R. H. French and Y.-M. Chiang, *J. Colloid Interf. Sci*., **179**, 460 (1996).
13. R. W. Carpick, D. F. Ogletree and M. Salmeron, *J. Colloid Interf. Sci*., **211**, 395 (1999).